

Compensation-dependence of magnetic and electrical properties in $\text{Ga}_{1-x}\text{Mn}_x\text{P}$

T. E. Winkler,^{1,2,3} P. R. Stone,^{1,2} Tian Li,³ K. M. Yu,^{1,2} A. Bonanni,^{3, a)} and O. D. Dubon^{1,2, b)}

¹⁾Department of Materials Science and Engineering, University of California, Berkeley, CA 94720, USA

²⁾Materials Sciences Division, Lawrence Berkeley National Laboratory, Berkeley, CA 94720, USA

³⁾Institut für Halbleiter- und Festkörperphysik, Johannes Kepler University, Altenbergerstraße 69, A-4040 Linz, Austria

(Dated: October 6, 2010)

We demonstrate the control of the hole concentration in $\text{Ga}_{1-x}\text{Mn}_x\text{P}$ over a wide range by introducing compensating vacancies. The resulting evolution of the Curie temperature from 51 K to 7.5 K is remarkably similar to that observed in $\text{Ga}_{1-x}\text{Mn}_x\text{As}$ despite the dramatically different character of hole transport between the two material systems. The highly localized nature of holes in $\text{Ga}_{1-x}\text{Mn}_x\text{P}$ is reflected in the accompanying increase in resistivity by many orders of magnitude. Based on variable-temperature resistivity data we present a general picture for hole conduction in which variable-range hopping is the dominant transport mechanism in the presence of compensation.

PACS numbers: 75.50.Pp, 72.80.Ey, 72.60.+g

Dilute magnetic semiconductors (DMSs), where a few atomic percent of magnetic ions are randomly substituted for a semiconductor host species, represent a remarkable workbench for the study and demonstration of spintronic functionalities.¹ They are not only a means to an end but very exciting materials in their own right, exhibiting many striking phenomena whose interpretation and modeling are extremely challenging – from the ferromagnetic exchange itself to the large anomalous Hall effect.² Much research has focused on III-Mn-V systems,^{2–5} where Mn acts as the source of both magnetic moment and carriers that mediate long-range ordering. While the behavior of $\text{Ga}_{1-x}\text{Mn}_x\text{As}$ is reasonably well understood at this point, the models developed in the process fall short of describing some other DMSs.²

$\text{Ga}_{1-x}\text{Mn}_x\text{P}$ is a prime candidate for further study, due to both its chemical similarity to $\text{Ga}_{1-x}\text{Mn}_x\text{As}$ as well as its low 0.36 % lattice mismatch with Si. Because the Mn acceptor level lies approximately four times deeper within the gap with respect to the valence band than in GaAs,⁶ the holes are of a much more localized nature. Still, hole-mediated ferromagnetism (FM) has been demonstrated conclusively in $\text{Ga}_{1-x}\text{Mn}_x\text{P}$ fabricated by ion implantation and pulsed-laser melting (II-PLM).⁷ In the best samples to date FM signatures persist up to a Curie temperature (T_C) of 65 K,⁸ which is 25 K lower than for $\text{Ga}_{1-x}\text{Mn}_x\text{As}$ at the same $x = 0.042$.⁹

One of the hallmarks of carrier-mediated FM is the dependence of the characteristic electrical, magnetic and optical properties on x and carrier (*i.e.*, hole) concentration, p . A major line of study pursued has thus been the behavior of $\text{Ga}_{1-x}\text{Mn}_x\text{P}$ over a range of x .^{8,10} While these samples implicitly exhibit different p as well, this approach only explores part of the available parameter space. Research into samples with constant x and varying p has been comparatively limited, focusing on anisotropy in S-codoped samples¹¹ and on T_C in S- and Te-codoped samples.^{7,12}

In this letter we present the first systematic study on the electrical and magnetic effects of hole compensation in $\text{Ga}_{1-x}\text{Mn}_x\text{P}$. We utilize the amphoteric nature of native defects¹³ – donor-like in $\text{Ga}_{1-x}\text{Mn}_x\text{P}$ ^{6,14} – to investigate a very wide range of p without significantly changing x . A similar method has recently been applied to $\text{Ga}_{1-x}\text{Mn}_x\text{As}$,¹⁵ and we find surprising similarities between the materials despite the radically different degree of hole localization. Furthermore, we present a picture for hole conduction by variable-range hopping (VRH) in $\text{Ga}_{1-x}\text{Mn}_x\text{P}$.

The samples for this study were prepared by II-PLM.¹⁶ A GaP (001) wafer – doped n-type; $n \sim 10^{16}\text{--}10^{17}\text{ cm}^{-3}$ – was implanted with Mn^+ at an energy of 50 keV and an angle of incidence of 7° to a dose of $2 \times 10^{16}\text{ cm}^{-2}$. Samples with approximate side lengths of 6 mm were cleaved along $\langle 110 \rangle$ directions and individually irradiated with a single $\sim 0.4\text{ J cm}^{-2}$ KrF laser pulse ($\lambda = 248\text{ nm}$, FWHM = 18 ns), homogenized to a spatial uniformity of $\pm 5\%$ by a crossed-cylindrical lens homogenizer. They were subsequently subjected to 24 h HCl etching to remove residual surface damage. These parameters have been used previously to produce samples with $x \approx 0.038$.⁸ For our samples, x is defined as the peak substitutional manganese (Mn_{Ga}) fraction – occurring between 20 and 30 nm below the surface – as determined by a combination of secondary ion mass spectrometry (SIMS) and ion beam analysis (IBA).¹⁷ Compensating defects were then introduced into samples by consecutive irradiations with Ar^+ at an energy of 33 keV and an angle of incidence of 7° , which according to simulations¹⁸ yield a vacancy depth profile similar to the typical Mn distribution.

The characterization of several identically prepared $\text{Ga}_{1-x}\text{Mn}_x\text{P}$ samples was carried out by SQUID magnetometry. All measurements were conducted in zero-field cooled conditions along the $[1\bar{1}0]$ in-plane magnetic easy axis,¹⁹ and the diamagnetic background was removed by linear fitting of variable-field magnetic moment $m(H)$ data up to $H = \pm 50\text{ kOe}$ at $T = 5\text{ K}$. They revealed an average saturation moment per Mn_{Ga} of $m_{\text{sub}}^{\text{sat}} = 3.7 \pm 0.4\ \mu_B$ in agreement with previous values.⁷ Temperature-dependent magnetic moment

^{a)}Electronic mail: alberta.bonanni@jku.at

^{b)}Electronic mail: oddubon@berkeley.edu

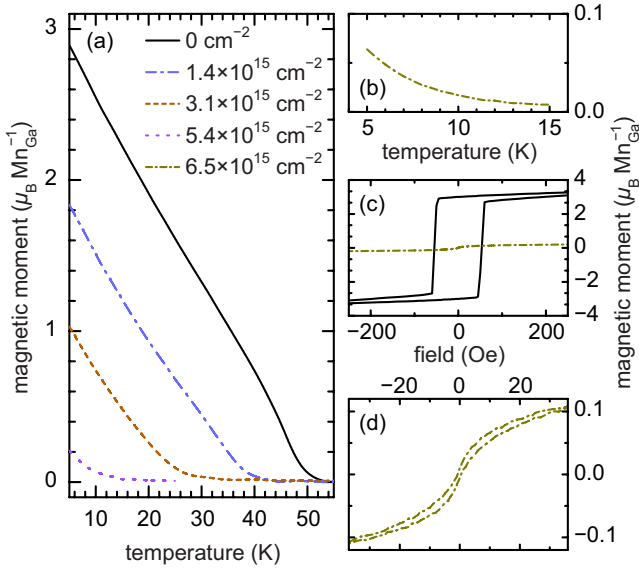


FIG. 1. (color online). (a) and (b) $m(T)$ at $H = 10 \text{ Oe}$ for various relative sheet hole concentrations Δp_s . (c) $m(H)$ at $T = 5 \text{ K}$ for as-fabricated and highest-dose irradiated films. (d) Magnetic hysteresis of the film at an irradiation dose of $5.77 \times 10^{12} \text{ cm}^{-2}$ (also shown in (c)).

$m(T)$ data at $H = 10 \text{ Oe}$ revealed $T_C = 50 \pm 1.5 \text{ K}$, which is well in line with both previous experimental⁸ and theoretical²⁰ results. Variable-temperature sheet resistance $\rho_s(T)$ measurements showed similar agreement between samples.

To confirm their structural integrity, samples were characterized after various irradiation doses. Using IBA, we found that the sheet concentration of Mn_{Ga} , c_s , remains constant within experimental errors and by SIMS that the Mn distribution is unaffected. High-resolution transmission electron microscopy and atomic force microscopy similarly show no qualitative changes with ion irradiation. Notably, even the sample with the highest irradiation dose shows no traces of secondary phases.

In order to track the degree of compensation, control samples were processed in parallel by implanting Zn^+ – a hydrogenic acceptor in GaP – to a dose of $1 \times 10^{16} \text{ cm}^{-2}$. On these, direct measurement of the hole concentration as a function of irradiation dose is possible using the Hall effect. From this data we have determined a hole removal rate of $1.1 \pm 0.1 \times 10^3$ holes per Ar^+ , or 2.2 ± 0.2 holes per vacancy when taking into account the simulations. Using this information, we calculate the relative sheet hole concentration Δp_s , defined as the difference in the sheet hole concentration p_s between the unirradiated reference and the irradiated sample.

In Fig. 1(a-b) we show $m(T)$ for various Δp_s , revealing a monotonic decrease of T_C with Δp_s . Similarly, we observe a decrease of $m_{\text{sub}}^{\text{sat}}$ with dose as evidenced in Fig. 1(c), consistent with previous studies of donor- or vacancy doping.^{11,15} We point out that this is in contrast to $m_{\text{sub}}^{\text{sat}}$ being unaffected by hydrogenation,^{22,23} indicating different mechanisms being involved in passivation *versus* compensation. The dependence of T_C on Δp_s is presented in Fig. 2, revealing a virtually

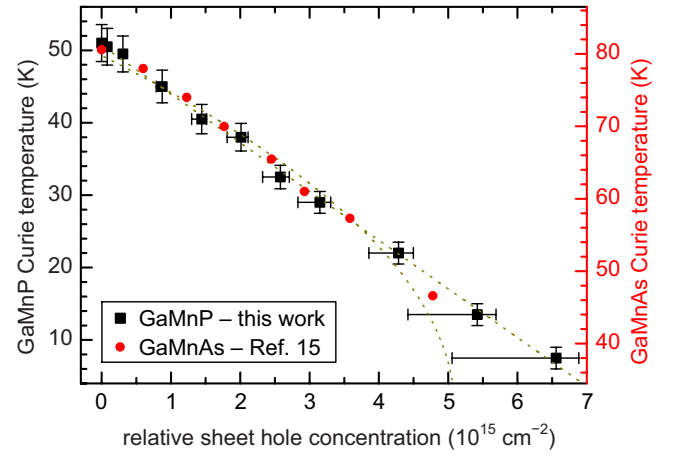


FIG. 2. (color online). T_C as a function of Δp_s for $\text{Ga}_{1-x}\text{Mn}_x\text{P}$ samples (squares, left scale) and $\text{Ga}_{0.955}\text{Mn}_{0.045}\text{As}$ samples (Ref. 15; circles, right scale). The asymmetric error bars for Δp_s reflect saturation effects of vacancy doping. The dotted lines are the simulated, limiting trends $T_C \propto p$ and $T_C \propto p^{0.5}$.

linear decline with decreasing hole concentration. We note that the highest irradiation dose of $5.77 \times 10^{12} \text{ cm}^{-2}$ should be sufficient to fully compensate the Mn acceptors, present at $c_s = 5.4 \pm 0.3 \times 10^{15} \text{ cm}^{-2}$. However, as apparent from Fig. 1(a-d), the films are FM at all irradiation doses, implying that they remain *p*-type even for the highest doses. This apparent discrepancy is explained by the amphoteric defect model (ADM),^{13,14} wherein the defect formation energy strongly depends on the Fermi level E_F , resulting in a saturation of the defect doping-induced shift in E_F at a material-dependent stabilization level E_{FS} . This effect becomes dominant in our system for $|\Delta p_s| \gtrsim 0.8 c_s$, considerations that are reflected in the error bars where appropriate. Furthermore, the persistence of FM even at these high levels of compensation demonstrates again that the compensation level of as-fabricated films must be very low.¹⁷

Accounting for the ADM-related compensation effects, we observe the relation $T_C \propto p^\gamma$ with $1 > \gamma > 0.5$ for $\text{Ga}_{1-x}\text{Mn}_x\text{P}$. Remarkably, such dependence of T_C on Δp_s is nearly identical to that observed in $\text{Ga}_{0.955}\text{Mn}_{0.045}\text{As}$ ¹⁵ films grown by low-temperature molecular beam epitaxy – that is, the trend is identical, barring a certain offset, reminiscent of the similarity in $T_C(x)$.²⁴ While our γ is in a similar range as a *p-d* Zener model prediction for $\text{Ga}_{1-x}\text{Mn}_x\text{As}$ of $\gamma = 0.6\text{--}0.8$,^{25,26} the model assumption of uniformly distributed delocalized or weakly localized holes does not apply to the $\text{Ga}_{1-x}\text{Mn}_x\text{P}$ films in this study.

$\rho_s(T)$ for $\text{Ga}_{1-x}\text{Mn}_x\text{P}$ samples with varying levels of compensation is displayed in Fig. 3. Films become orders of magnitude more resistive with increasing irradiation dose.

The generally applied, phenomenological model in $\text{Ga}_{1-x}\text{Mn}_x\text{P}$ has been $\rho = (\sigma_{\text{free}} \exp(-\varepsilon_1/k_B T) + \sigma_{\text{hop}} \exp(-\varepsilon_3/k_B T))^{-1}$.⁷ Here the first term is attributed to thermally activated hole transport *via* the valence band and the second term to hopping conduction, previously assumed

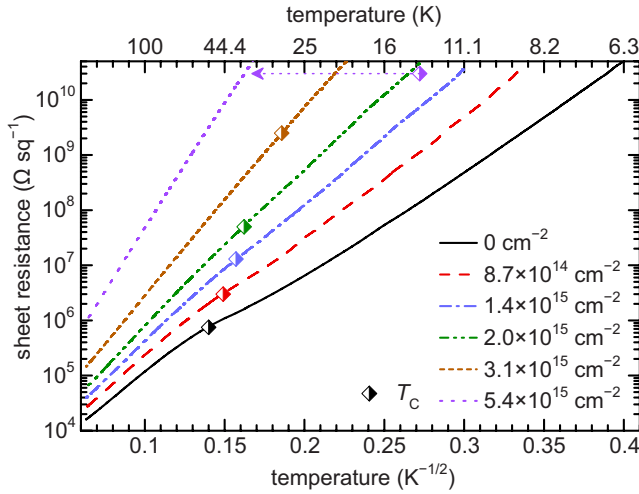


FIG. 3. (color online). ρ_s of $\text{Ga}_{1-x}\text{Mn}_x\text{P}$ versus $T^{-1/2}$ for various relative sheet hole concentrations Δp_s . T_C is indicated for each dose by a diamond, for the highest Δp_s supplemented by an arrow.

to take place between nearest neighbors.^{12,27,28} This model reproduces the behavior of samples with varying x which have not been intentionally compensated.⁸ For the current case of compensated films, however, we find overall better agreement with activated transport of the form $\rho \propto \exp(\varepsilon T^\lambda)$ with a temperature exponent of $\lambda \sim -0.5$, separated into a high- and a low-temperature regime characterized by different activation energies ε . We attribute the general behavior to hopping conduction, specifically VRH.²⁸ That this mechanism should dominate even at high T for large Δp_s is reasonable as the energetic difference between delocalized states and E_F – here on the order of the Mn acceptor level of 0.4 eV⁶ – can easily be an order of magnitude larger than $k_B T$. At $\Delta p_s \lesssim 10^{15} \text{ cm}^{-2}$, VRH is insufficient to describe fully the transport at high T . In this regime, the conduction by holes excited thermally to delocalized states, as described previously,⁷ contributes or even dominates. This behavior is qualitatively similar to that observed in insulating, low-doped $\text{Ga}_{1-x}\text{Mn}_x\text{As}$ ²⁹ and even more so to that in insulating, Sn-codoped $\text{Ga}_{1-x}\text{Mn}_x\text{As}$.³⁰

In conclusion, the orders-of-magnitude changes in conductivity and the much more subtle changes in the magnetic response upon compensation using Ar^+ -induced native defects demonstrate the stability of the hole-mediated FM phase in $\text{Ga}_{1-x}\text{Mn}_x\text{P}$. While the electrical behavior of $\text{Ga}_{1-x}\text{Mn}_x\text{P}$ and $\text{Ga}_{1-x}\text{Mn}_x\text{As}$ at comparable x is dramatically different, these materials display a remarkably similar T_C dependence on both hole concentration and Mn content. This indicates similar mechanisms for inter-Mn exchange in the two systems and places carrier-mediated FM on a continuum of carrier localization in III-Mn-V DMSs.

ACKNOWLEDGMENTS

The work at Berkeley (sample synthesis, electrical and magnetic characterization, ion beam analysis) was supported by the Director, Office of Science, Office of Basic Energy Sciences, Division of Materials Sciences and Engineering, of the U.S. Department of Energy under Contract No. DE-AC02-05CH11231. The work at Linz (structural characterization) was supported by the European Research Council through the FunDMS Advanced Grant within the “Ideas” 7th Framework Programme of the EC, and by the Austrian Fonds zur Förderung der wissenschaftlichen Forschung – FWF (Grants P22477, P20065, and N107-NAN). We thank R. Jakiela for SIMS measurements. P.R. S. acknowledges support from an NSF fellowship, T.E. W. from a Marshall Plan Scholarship.

REFERENCES

1. T. Dietl, D. D. Awschalom, M. Kamińska, and H. Ohno, *Spintronics*, edited by E. R. Weber, Semiconductors and Semimetals, Vol. 82 (Elsevier, Amsterdam, 2008).
2. T. Jungwirth, J. Sinova, J. Mašek, J. Kučera, and A. H. MacDonald, *Rev. Mod. Phys.* **78**, 809 (2006).
3. F. Matsukura, H. Ohno, and T. Dietl, in *Handbook of Magnetic Materials*, Vol. 14, edited by K. H. J. Buschow (Elsevier, Amsterdam, 2002) pp. 1–87.
4. K. S. Burch, D. D. Awschalom, and D. N. Basov, *J. Magn. Magn. Mater.* **320**, 3207 (2008).
5. K. Sato, L. Bergqvist, J. Kudrnovský, P. H. Dederichs, O. Eriksson, I. Turek, B. Sanyal, G. Bouzerar, H. Katayama-Yoshida, V. A. Dinh, T. Fukushima, H. Kizaki, and R. Zeller, *Rev. Mod. Phys.* **82**, 1633 (2010).
6. B. Clerjaud, *J. Phys. C* **18**, 3615 (1985).
7. M. A. Scarpulla, B. L. Cardozo, R. Farshchi, W. M. Hlaing Oo, M. D. McCluskey, K. M. Yu, and O. D. Dubon, *Phys. Rev. Lett.* **95**, 207204 (2005).
8. R. Farshchi, M. A. Scarpulla, P. R. Stone, K. M. Yu, I. D. Sharp, J. W. Beeman, H. H. Silvestri, L. A. Reichertz, E. E. Haller, and O. D. Dubon, *Solid State Commun.* **140**, 443 (2006).
9. T. Jungwirth, K. Y. Wang, J. Mašek, K. W. Edmonds, J. König, J. Sinova, M. Polini, N. A. Goncharuk, A. H. MacDonald, M. Sawicki, A. W. Rushforth, R. P. Campion, L. X. Zhao, C. T. Foxon, and B. L. Gallagher, *Phys. Rev. B* **72**, 165204 (2005).
10. P. R. Stone, M. A. Scarpulla, R. Farshchi, I. D. Sharp, E. E. Haller, O. D. Dubon, K. M. Yu, J. W. Beeman, E. Arenholz, J. D. Denlinger, and H. Ohldag, *Appl. Phys. Lett.* **89**, 012504 (2006).
11. P. R. Stone, C. Bihler, M. Kraus, M. A. Scarpulla, J. W. Beeman, K. M. Yu, M. S. Brandt, and O. D. Dubon, *Phys. Rev. B* **78**, 214421 (2008).
12. M. A. Scarpulla, P. R. Stone, I. D. Sharp, E. E. Haller, O. D. Dubon, J. W. Beeman, and K. M. Yu, *J. Appl. Phys.* **103**, 123906 (2008).
13. W. Walukiewicz, *Appl. Phys. Lett.* **54**, 2094 (1989).
14. W. Walukiewicz, *Phys. Rev. B* **37**, 4760 (1988).
15. M. A. Mayer, P. R. Stone, N. Miller, H. M. Smith, O. D. Dubon, E. E. Haller, K. M. Yu, W. Walukiewicz, X. Liu, and J. K. Furdyna, *Phys. Rev. B* **81**, 045205 (2010).
16. M. A. Scarpulla, O. D. Dubon, K. M. Yu, O. Monteiro, M. R. Pillai, M. J. Aziz, and M. C. Ridgway, *Appl. Phys. Lett.* **82**, 1251 (2003).
17. P. R. Stone, M. A. Scarpulla, K. M. Yu, and O. D. Dubon, in *Handbook of Spintronic Semiconductors*, edited by W. M. Chen and I. A. Buyanova (Pan Stanford Publishing, Singapore, 2010).
18. J. F. Ziegler, M. D. Ziegler, and J. P. Biersack, “SRIM 2008.04,” <http://www.srim.org/> (2008).
19. C. Bihler, M. Kraus, H. Huebl, M. S. Brandt, S. T. B. Goennenwein, M. Opel, M. A. Scarpulla, P. R. Stone, R. Farshchi, and O. D. Dubon, *Phys. Rev. B* **75**, 214419 (2007).
20. H. Katayama-Yoshida, K. Sato, T. Fukushima, M. Toyoda, H. Kizaki, V. A. Dinh, and P. H. Dederichs, *Phys. Status Solidi A* **204**, 15 (2007).

- ²¹See supplementary material at [URL will be inserted by AIP] for SIMS and IBA data.
- ²²C. Bihler, M. Kraus, M. S. Brandt, S. T. B. Goennenwein, M. Opel, M. A. Scarpulla, R. Farshchi, D. M. Estrada, and O. D. Dubon, *Journal of Applied Physics* **104**, 013908 (2008).
- ²³S. T. B. Goennenwein, T. A. Wassner, H. Huebl, M. S. Brandt, J. B. Philipp, M. Opel, R. Gross, A. Koeder, W. Schoch, and A. Waag, *Phys. Rev. Lett.* **92**, 227202 (2004).
- ²⁴P. R. Stone, K. Alberi, S. K. Z. Tardif, J. W. Beeman, K. M. Yu, W. Walukiewicz, and O. D. Dubon, *Phys. Rev. Lett.* **101**, 087203 (2008).
- ²⁵Y. Nishitani, D. Chiba, M. Endo, M. Sawicki, F. Matsukura, T. Dietl, and H. Ohno, *Phys. Rev. B* **81**, 045208 (2010).
- ²⁶T. Dietl, H. Ohno, and F. Matsukura, *Phys. Rev. B* **63**, 195205 (2001).
- ²⁷A. Kaminski and S. Das Sarma, *Phys. Rev. B* **68**, 235210 (2003).
- ²⁸B. I. Shklovskii and A. L. Efros, *Electronic Properties of Doped Semiconductors*, Solid-State Sciences, Vol. 45 (Springer, Berlin, 1984).
- ²⁹B. L. Sheu, R. C. Myers, J.-M. Tang, N. Samarth, D. D. Awschalom, P. Schiffer, and M. E. Flatté, *Phys. Rev. Lett.* **99**, 227205 (2007).
- ³⁰Y. Satoh, D. Okazawa, A. Nagashima, and J. Yoshino, *Physica E* **10**, 196 (2001).